## CHAPTER 4

# The Approximate Scalar Potential: Properties and Shortcomings

The question now on our agenda: Assuming we have solved the linear system (20) in Chapter 3, and thus obtained the vector $\boldsymbol{\varphi}$ of nodal potentials, to what extent is the approximate solution $\varphi_m = \sum_{n \in \mathcal{N}} \boldsymbol{\varphi}_n \lambda^n$ satisfactory as a representation of the field? On the side of h, all goes well: Setting $h_m = \text{grad}\ \varphi_m$, we have $\text{rot}\ h_m = 0$ as well as $n \times h_m = 0$ on $S^h$ and $\int_c \tau \cdot h_m = I$, all that by construction. Errors are on the side of b: We lose solenoidality of $b_m = \mu h_m$, since not all test functions have been retained. Some measure of flux conservation still holds, however, and we'll see in which precise sense. When the mesh is refined, we expect to recover $\text{div}\ b = 0$ "at the limit"; this is the issue of *convergence*. But how *fast* do $h_m$ and $b_m$ converge toward h and b, and how *far* apart are they in energy? These are related questions, but the latter is more difficult and will not be resolved before Chapter 6. Last, there is a property of the true solution, expressed by the so-called *maximum principle*, which may be preserved to some extent, provided the mesh is carefully devised, and Voronoi–Delaunay meshes seem to be adequate in this respect.

### 4.1 THE "*m*-WEAK" PROPERTIES

Last chapter, we defined "discrete" or "*m*-weak" solenoidality as the property

(1) $\qquad \int_D b \,.\, \text{grad}\ \varphi' = 0 \quad \forall\, \varphi' \in \Phi^0{}_m$,

that is, with nodal finite elements, $\int_D b \cdot \text{grad}\ \lambda^n = 0$ for all n in the subset $\mathcal{N}_0 = \mathcal{N} - \mathcal{N}(S^h)$. We shall dub *active* the nodes of this set, which

includes inner nodes (i.e., not on $S$) and surface nodes interior to $S^b$, but not those at the boundary common to $S^b$ and $S^h$, where nodal values are imposed. Active nodes are those which bear an unknown degree of freedom, and each of them corresponds to a row of the submatrix ${}^{00}\mathbf{M}$ of Eq. (3.20).

### 4.1.1 Flux losses

Condition (1) is much less stringent than weak solenoidality, so what is left of $\mathrm{div}\, b = 0$? In the worst case, nothing: $h_m$ is constant inside a tetrahedron, so if $\mu$ varies, then $\mathrm{div}(\mu h_m) = \nabla\mu \cdot h_m$, which has no reason to vanish. But this is easily cured: Replace $\mu$, either *before* the computation of $\mathbf{M}$ by (3.19), or at the stage we consider now, by a mesh-wise constant function $\bar{\mu}$, equal to $(\int_T \mu)/\mathrm{vol}(T)$ on tetrahedron $T$. Then $b_m = \bar{\mu} h_m$, being mesh-wise constant, is solenoidal inside each $T$. Can we expect its normal jumps $[n \cdot b_m]_f$, which are a priori constant over each face of the mesh, to vanish, all of them? By no means, because that would make $b_m$ divergence-free and enforce $n \cdot b_m = 0$ on $S^b$. Thereby, all the equations of the continuous model would be satisfied by the discrete model (in the case of a mesh-wise constant $\mu$), which would then yield the right solution, and such miracles are not to be expected. Jumps of $n \cdot b_m$ don't vanish, so there is a "loss of induction flux", equal to the integral of this jump, at each inter-element boundary.

This prediction is confirmed by comparatively counting these lost fluxes and the equations. We have $N$ nodes, $E$ edges, $F$ faces and $T$ tetrahedra. By a famous result in topology to which we shall return, one has

$$N - E + F - T = \chi,$$

where $\chi$, the *Euler–Poincaré* constant, which a priori seems to depend on $m$, is actually determined by the global topological properties of $D$. It's a small integer, typically 1 for simple domains. (**Exercise 4.1:** Compute $\chi$ for a single tetrahedron and for a meshed cube.) Assume a typical mesh, made by first generating hexahedra, then chopping them into six tetrahedra each (cf. Exer. 3.7). Then $T \sim 6N$, and $F \sim 12N$, since each tetrahedron has four faces that, most of them, belong to two tetrahedra, hence $E \sim 7N$. Having about $N$ degrees of freedom, we can't satisfy $F \sim 12N$ constraints—but wait, are there really $F$ lost fluxes to cancel? No, because the fluxes through faces of a same tetrahedron add to zero, since $\mathrm{div}\, b_m = 0$ inside. So there are about $F - T$ *independent* lost fluxes to consider. Still, this is about $E - N$, much larger than $N$.

We must therefore accept nonzero jumps of $n \cdot b$ through faces as a weakness inherent in the method: $b_m$ is not, as one says, "div-conformal". (The latter expression does not mean "solenoidal": A field is *div-conformal* when its normal component is continuous through all surfaces, which is a weaker condition.) So the approximate solution fields will *not* satisfy the "law of tangents" of (2.5), and indeed, in two-dimensional simulations, it's fairly common to see flux lines that behave "wrongly", as shown in the inset, staying on the same side of the normal to an edge when going from one triangle to the next.[1] We are used to that nowadays, knowing this is the price to pay for having a *finite* system of equations to solve instead of the *infinite* system that Problem (3.1) represented, and we can rely on the assurance that with refinement of the mesh, such non-physical behavior of flux lines will disappear (a proof to this effect will come). But in the early days of the finite element method, this feature was met with harsh criticism, touching off a controversy, some echoes of which can be found in [CS, EF, FE].

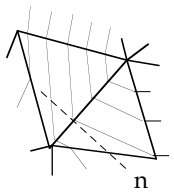


**Remark 4.1.** A nonzero jump of $n \cdot b$ at element interfaces is equivalent to the presence of a magnetic charge density $[n \cdot b]$ there. Thus, $b_m$ can be described as the induction field that would appear if these fictitious charges were really present, in addition to the external sources of the field. ◊

Let us therefore try to assess the damage as regards these inevitable flux losses, or spurious charges. This will depend on an interpretation of each component of the vector $\mathbf{M}\boldsymbol{\varphi}$, as follows.

First, let us consider any DoF vector $\boldsymbol{\varphi}$, *not* related to the solution. We form the mesh-wise affine function[2] $\varphi = p_m(\boldsymbol{\varphi}) = \sum_{n \in \mathcal{N}} \boldsymbol{\varphi}_n \lambda^n$, and the vector field $b = \bar{\mu}\ \text{grad}\ \varphi$. Note that $b$ is mesh-wise constant. By the very definition of $\mathbf{M}$,

$$(\mathbf{M}\boldsymbol{\varphi})_n \equiv \sum_{m \in \mathcal{N}} \mathbf{M}_{nm} \boldsymbol{\varphi}_m = \int_D b \cdot \text{grad}\, \lambda^n.$$

Integrating by parts on each tetrahedron, and summing up, one obtains (sorry for the clash of n's):

$$(2) \qquad (\mathbf{M}\boldsymbol{\varphi})_n = \sum_{f \in \mathcal{F}(n)} \int_f [n \cdot b]\, \lambda^n = \tfrac{1}{3} \sum_{f \in \mathcal{F}(n)} \int_f [n \cdot b]\,,$$

[1] Curiously, the bending of flux lines across mesh edges, which is just as "unphysical" in a homogeneous region, was not regarded as scandalous when the normal was properly crossed by flux lines.

[2] The notation $p_m$ has been introduced in Subsection 3.3.3.

because the jump is constant over f, and the average of $\lambda^n$ over f is equal to $1/3$ (Exer. 3.9). For further reference, let's give a name to $(\mathbf{M}\boldsymbol{\varphi})_n$, the component of $\mathbf{M}\boldsymbol{\varphi}$ at node n, and call it the *flux loss at*, or *about* node n, as regards b. After (2), this loss is one-third of the sum of flux losses at faces that have n as common node (face set $\mathcal{F}(n)$).

There is another interpretation of this flux loss, for which it will be convenient to distinguish inner nodes and surface nodes. If n is an interior node, the faces of $\mathcal{F}(n)$ are the "inner faces" of the cluster (the opaque ones in the inset drawing). Since b is mesh-wise constant, $\int_{\partial T} n \cdot b = 0$ for all tetrahedra. The sum of these terms over all tetrahedra of the cluster is also the sum of the outward flux through the cluster's boundary and of the inner flux losses. Therefore, the flux loss at n is one third of the flux entering its cluster. The same argument works if n belongs to the surface: Then n lies on the polyhedral boundary of its own cluster (Fig. 4.1), and the flux loss at n is one-third of the flux entering the "polyhedral cap" of n, as sketched in Fig. 4.1, right.

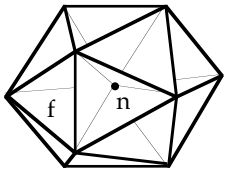


Now, consider the case when $\boldsymbol{\varphi}$ is the solution of the discrete problem, Eq. (3.20). Row n of this linear system corresponds, equivalently, to

$$(3) \qquad \int_{D_n} b_m \cdot \operatorname{grad} \lambda^n = 0, \qquad (3') \qquad (\mathbf{M}\boldsymbol{\varphi})_n \equiv \sum_{m \in \mathcal{N}(n)} \mathbf{M}_{n\,m}\, \boldsymbol{\varphi}_m = 0.$$

So discrete solenoidality entails the cancellation of all flux losses of $b_m$ at active nodes. Therefore, by what precedes, the *fluxes of* $b_m$ *through the surface of the cluster of each inner node* and *through the cap of each active boundary node* must vanish.

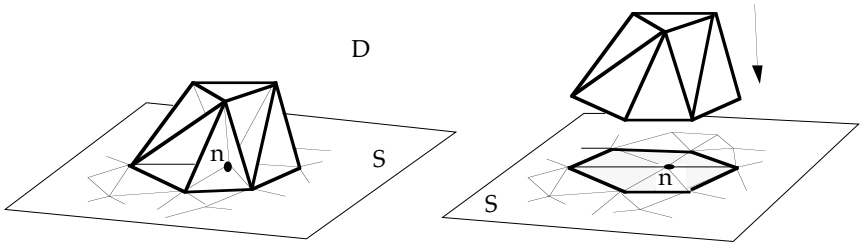


**FIGURE 4.1.** Left: Cluster of tetrahedra around a boundary node (D here is above the triangulated plane). Inner faces of the cluster are opaque; others are transparent. Right: Dissecting the cluster's boundary into a "patch" of boundary triangles around n, and a "cap" of inside faces.

Note that we *don't* find $n \cdot b_m = 0$ on faces of $S^b$. Actually, we had no reason to entertain such hopes, since there are about twice[3] as many faces as nodes on $S^b$, thus not enough equations to cancel all these fluxes.

It's very tempting to try and combine these results by merging clusters of different nodes into larger clusters, and to say, "Well, just as the flux of the true solution $b$ is null for all closed surfaces inside $D$ (remember, this is the integral interpretation of weak solenoidality), the flux of $b_m$ through polyhedral surfaces made of mesh-faces will vanish." Fine guesswork . . . but wrong, as the following exercise will show.

**Exercise 4.2.** In dimension 2, suppose $b_m$ satisfies (3) over a domain that contains the two "extended clusters" of Fig. 4.2. Show that the flux through $\Sigma_1$ or $\Sigma_2$ does not vanish.

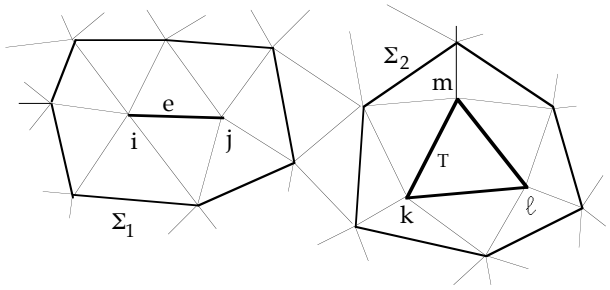


**FIGURE 4.2.** Part of a 2D mesh $m$ by which a discretely solenoidal induction $b_m$ has been computed. Although the flux of $b_m$ through cluster boundaries vanishes, it does not on the boundaries $\Sigma_1$ or $\Sigma_2$ of extended clusters, that is, unions of clusters of node subsets such as {i, j} or {k, ℓ, m}.

And yet there is something correct in this intuition. But we need relatively sophisticated new concepts to develop this point.

### 4.1.2 The dual mesh, and which fluxes are conserved

First, the *barycentric refinement* of a simplicial mesh $m$. This is a new simplicial mesh, which we shall denote by $m/2$, obtained as suggested by Fig. 4.3: Add one node at each mid-edge and at the center of gravity of each face and each tetrahedron, subdivide, and add edges and faces as

[3]It's Euler–Poincaré again, for surfaces this time: N – E + F = χ, and 2E ~ 3F. Things may seem different in dimension 2, where there are almost as many boundary nodes as boundary *edges* (the difference is the number of connected components of $S^h$). Still, even when these numbers coincide, there is no reason to expect fluxes at boundary edges to be exactly zero.

required. Visualizing it in dimension 2 is easy (Fig. 4.3), but it takes some imagination in three dimensions.

Next, the *dual* mesh (the primitive one then being referred to as the *primal* mesh). The dual mesh is not a simplicial mesh, but what can be called a "cellular" tessellation, the cells being polyhedra, polyhedral surfaces, broken lines (Fig. 4.4), and points. The 3-cells, one for each primal node, are clusters of tetrahedra around n, but tetrahedra of the subdivided mesh $m/2$, not of $m$. Such a shrunk cluster (see Fig. 4.3 for one in dimension 2) is informally called a "box". Fig. 4.4 shows a part of the box around n, the part that intersects tetrahedron T. Two-cells are associated with edges: The 2-cell of edge e is the union of all faces of $m/2$ that contain the midpoint of e, but none of its extremities (Fig. 4.4). Note that it's not a *plane* polygon (though its parts within each tetrahedron are plane). One-cells, associated with faces, are unions of the two segments which join the barycenter of a face to those of the two tetrahedra flanking it. And 0-cells, the nodes of the dual mesh, are centers of gravity of the primal tetrahedra.

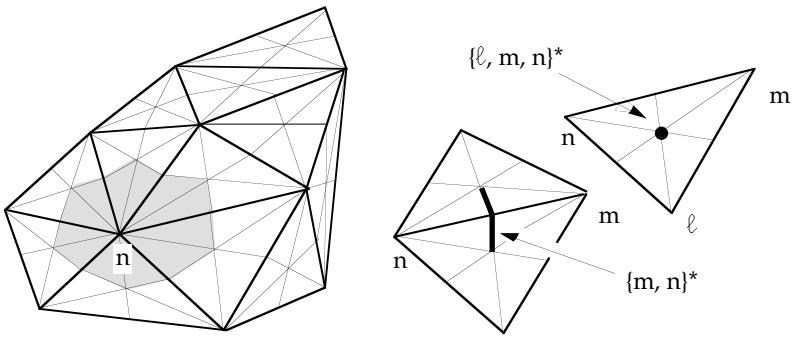


**FIGURE 4.3.** Barycentric refinement of a 2D mesh. Thick edges are those of the primitive mesh. Shaded, the "box", or "dual 2-cell" around node n. Right: dual cells (for 3D examples, see Fig. 4.4).

There is thus a perfect duality between the two meshes, p-simplices of $m$ being in one-to-one correspondence with (d – p)-cells of the dual mesh, where d is the spatial dimension. We may denote the dual mesh by $m^*$, and play on this notation: the box around n can be denoted $n^*$ (but we'll call it $B_n$), the corolla of small faces around edge e is $e^*$, etc. Note that—this is clear in Fig. 4.3, but valid in all dimensions—dual p-cells intersect along dual q-cells, with $q < p$. In particular, the common boundary of two adjacent boxes is the dual 2-cell of the edge joining their nodes. (**Exercise 4.3:** When do two dual 2-cells intersect at a point? Along a line?)

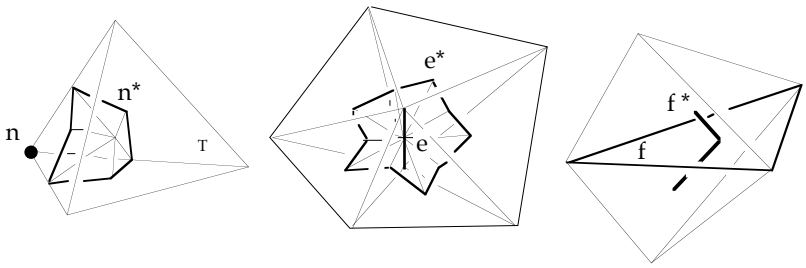


**FIGURE 4.4.** Cells of the dual mesh $m^*$: All dual p-cells are unions of p-simplices of the barycentric refinement of $m$. From left to right, a part of the box $n^*$, a 2-cell $e^*$ around edge e, and a 1-cell $f^*$ through face f.

Finally, for further use, let us define something we shall call, for shortness, *$m^*$-surfaces:* Surfaces, with or without boundary, made of dual 2-cells. Box surfaces are $m^*$-surfaces (after removing the part that may lie in S), and the surface of a union of boxes is one, too. Similarly, of course, we have *$m^*$-points* (nodes of the dual mesh, i.e., centers of tetrahedra), *$m^*$-lines* (made of dual 1-cells), and *$m^*$-volumes* (unions of boxes).

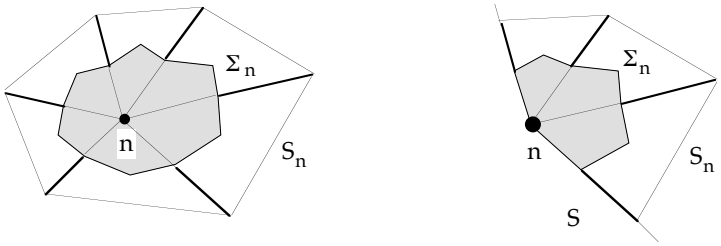


**FIGURE 4.5.** Comparing the fluxes through $\Sigma_n$ and $S_n$. (Beware, this is a 2D representation, in which surfaces $\Sigma_n$, $S_n$, S appear as lines.)

With this, we can refine our interpretation of $\mathbf{M}\boldsymbol{\varphi}$. Again, given some DoF vector $\boldsymbol{\varphi}$, form $\varphi = p_m(\boldsymbol{\varphi})$ and $b = \overline{\mu}\ \mathrm{grad}\,\varphi$. Then,

**Proposition 4.1.** *The term* $(\mathbf{M}\boldsymbol{\varphi})_n = \int_D b \cdot \mathrm{grad}\,\lambda^n$, *or flux loss of* b *about* n, *is the inward flux of* b *across the surface of the box around* n, *if* n *is an inner node, and across the "$m^*$-cap" of Fig. 4.5, if* n *is a surface node.*

*Proof.* Since b is divergence-free inside tetrahedra, the difference between its fluxes through the cluster surface $S_n$ and through the box surface $\Sigma_n$ is due to flux leaks at the parts of inner faces of the cluster which are in the shell between $\Sigma_n$ and $S_n$ (thick lines in the 2D drawing). But for each such face, exactly two-thirds of its area are there (in dimension 2, and on the drawing, one-half of the edge length). And since jumps of $n \cdot b$ are constant over each face, the total of these flux leaks in the shell is thus

two-thirds of the total of flux leaks in the cluster. The remaining third is thus the flux through $\Sigma_n$. Same reasoning if $n$ belongs to the boundary, $\Sigma_n$ now being the "$m$*-cap" over $n$ (smaller than the cap of Fig. 4.1) made of dual 2-cells. ◊

**Remark 4.2.** One cannot overstress the importance of having a *barycentric* subdivision to get this result; the uniformity of the ratio $2/3$ between areas was essential. ◊

In other words, $(\mathbf{M}\boldsymbol{\varphi})_n$ is the part of the flux of $b$ entering box $B_n$ that comes from other boxes, and the entries of $\mathbf{M}$ govern fluxes between boxes in a very simple way: $B_m$ gives $\mathbf{M}_{n\,m}(\boldsymbol{\varphi}_m - \boldsymbol{\varphi}_n)$ to $B_n$. The finite element method thus appears as simple bookkeeping of induction flux exchanges between boxes, or "finite volumes", in which the computational domain has been partitioned. Exercise 4.4 at the end is an invitation to follow up on this idea.

With this, we can return to the characterization of $b_m$: Its flux through the box surface of an inner node, or through the small cap of an active surface node, vanishes. Since inter-box boundaries are always *inside* tetrahedra, where $b_m$ is solenoidal, there are no flux leaks at such interfaces, so we may aggregate boxes, and the flux entering such an aggregate is the sum of flux losses at all nodes inside it. Therefore, the flux of $b_m$ will vanish across polyhedral surfaces of two kinds: $m$*-surfaces that enclose one or several boxes around inner nodes, and "extended $m$*-caps", covering one or several $S^b$-nodes.

To make sense out of this, let's compare the present "discrete" situation to the "continuous" one. In the latter, the flux of the true solution $b$ is null for all closed surfaces inside $D$ which enclose a volume (this is the integral interpretation of weak solenoidality), and also, since $n \cdot b = 0$ on $S^b$, for all surfaces with boundary which, with the help of $S^b$, enclose a volume. So it goes exactly the same in the discrete situation, except that surfaces must be made of dual 2-cells. All this cries out for the introduction of new definitions, if only for ease of expression:

**Definition 4.2.** *Let* $C$ *be a part of* $D$. *A surface in* $\overline{D}$ *is* closed modulo $C$ *if its boundary is in* $C$. *A surface* $\Sigma$ bounds modulo $C$ *if there is a volume* $\Omega$ *contained in* $\overline{D}$ *such that* $\partial\Omega - \Sigma$ *is in* $C$.

Same concepts[4] for a line $\sigma$, which is *closed mod* $C$ if its end-points are in $C$, and *bounds mod* $C$ if there is a surface $\Gamma$ such that $\partial\Gamma - \sigma$ is in $C$.

[4]Lines and surfaces can be in several pieces, but trying to formalize that, via the concept of *singular chain*, would lead us too early and too far into *homology* [GH, HW]. (Don't confuse the present notion of closedness with the topological one; cf. A.2.3.)

Figure 4.6 gives a few examples. (As one sees, what is often called informally a "cutting surface" or "cut" is a closed surface (mod. something) that doesn't bound. Cf. Exer. 2.6.)

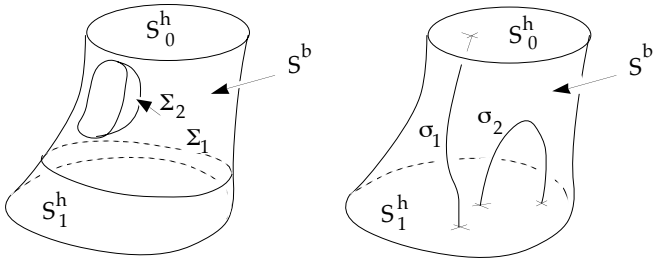


**FIGURE 4.6.** Left: Surfaces $\Sigma_1$ and $\Sigma_2$ are both closed modulo $S^b$, but only the latter bounds mod $S^b$. Right: Lines $\sigma_1$ and $\sigma_2$ are both closed modulo $S^h$, but only the latter bounds mod $S^h$.

Thus equipped, we can reformulate our findings. The conditions about b, in the continuous model, were that $\int_\Sigma n \cdot b = 0$ for all surfaces $\Sigma$ which bound modulo $S^b$. In contrast, and in full recovery from our earlier fiasco, we have obtained this:

**Proposition 4.2.** *The discretized field satisfies* $\int_\Sigma n \cdot b_m = 0$ *for all m*-surfaces* $\Sigma$ *which bound modulo* $S^b$.

**Exercise 4.5.** What if there are flux sources inside the domain (cf. Exers. 2.8 and 3.1) ?

### 4.1.3 The flux through $S^h$

The aim of our modelling was supposed to be the reluctance $R = I/F$, so we need the induction flux $F$ through the domain in terms of $\boldsymbol{\varphi}$.

Following the hint of Remark 3.2, one has

$$\int_D \mu \, |\operatorname{grad} \varphi|^2 = \int_D b \cdot \operatorname{grad} \varphi = \int_S n \,.\, b\varphi = I \int_{S^h_1} n \cdot b = I\,F,$$

if $\varphi$ is the exact solution. Since $\mathbf{(M\varphi, \varphi)}$ is by construction the best approximation we have for $\int_D \mu \, |\operatorname{grad} \varphi|^2$, the best estimate for $F$ is the mesh-dependent ratio $F_m = \mathbf{(M\varphi, \varphi)}/I$, hence an approximation $R_m$ of the reluctance in our model problem: $R_m = I^2/\mathbf{(M\varphi, \varphi)}$, of which we may remark it is *by default*—from below—since $\mathbf{(M\varphi, \varphi)}$, being obtained by minimizing on too small a space, exceeds the infimum of $\int_D \mu \, |\operatorname{grad} \varphi|^2$. We'll return to this in Chapter 6.

Developing $\mathbf{(M\varphi, \varphi)}$, we see that

$$F_m = I^{-1} \sum_{n \in \mathcal{N}} (\mathbf{M}\boldsymbol{\varphi})_n \, \boldsymbol{\varphi}_n = \sum \{ (\mathbf{M}\boldsymbol{\varphi})_n : n \in \mathcal{N}(S^h_1) \},$$

since $(\mathbf{M}\boldsymbol{\varphi})_n = 0$ for all nodes $n \in \mathcal{N}_0$ and $\boldsymbol{\varphi}_n = 0$ or I for n in $\mathcal{N}(S^h_0)$ or $\mathcal{N}(S^h_1)$. The flux is therefore approximated by the sum of flux losses at points of $S^h_1$, which is equal, after Prop. 4.1 (aggregate the boxes of all points of $S^h_1$), to the flux at the surface $\Sigma$ of Fig. 4.7 (seen as a broken line in this 2D sketch), obtained by merging the small caps ($m$*-caps) of all nodes of $S^h_1$.

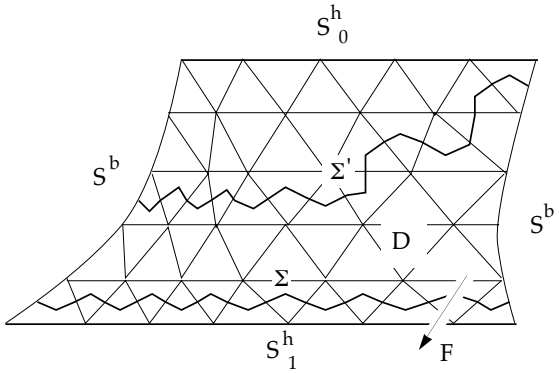


**FIGURE 4.7.** Where to compute the flux of $b_m$.

**Exercise 4.6.** What about $m$*-surfaces like $\Sigma'$ in Fig. 4.7? Show that the flux of $b_m$ is the same through all of those which are homologous to $\Sigma$, in the sense of Exer. 2.6.

As one sees, the "variationally correct" approximation of the flux is not what a naive approach would suggest, that is, $\int_{S^h_1} \mu \, \partial_n(p_m(\boldsymbol{\varphi}))$, but the same integral taken over $\Sigma$ (or any $m$*-surface homologous to it) instead of $S^h_1$. One should not, in consequence, use $\mu \, \partial_n(p_m(\boldsymbol{\varphi}))$ as approximation for the normal induction, but treat the latter, for all purposes, as a surface distribution $\varphi' \to \int_S \mu \, \partial_n\varphi \, \varphi'$, and use the scalar product $(\mathbf{M}\boldsymbol{\varphi}, \boldsymbol{\varphi}')$ as approximation of this integral, with $\boldsymbol{\varphi}'_n = \varphi'(x_n)$. (Cf. Exer. 4.8.)

**Exercise 4.7.** In which sense is $\mathbf{M}$ a discrete analogue of the differential operator $-\operatorname{div}(\mu \operatorname{grad})$?

**Exercise 4.8.** Suppose one solves a problem similar to our model problem, but with $\varphi$, for some reason, equal to a given boundary data $\varphi^h$ on $S^h$. Write down the best estimate of the functional $\int_D \mu \, |\operatorname{grad} \varphi|^2$ in terms of the DoFs on $S^h$. (This way of expressing the energy inside a region in terms of boundary values of the field is a very useful procedure, known as "static condensation" in mechanics. Can you find a better denomination, more germane to electromagnetism?)

## 4.2 THE MAXIMUM PRINCIPLE

If $\Delta\varphi = 0$ in some domain, $\varphi$ cannot reach its maximum or minimum elsewhere than on the *boundary* of the domain. This is the *maximum principle* for harmonic functions. A similar property holds for the magnetic potential, and some of it may be retained at the discrete level.

### 4.2.1 Discrete maximum principle

Let's recall the proof. First (an easy assignment):

**Exercise 4.9.** Show that the function $y \to (4\pi\,|x-y|)^{-1}$ is harmonic in $E_3 - \{x\}$.

Next, suppose $\mathrm{div}(\mathrm{grad}\,\varphi) = 0$ in some domain D. Consider two spheres S(x, r) and S(x, R) contained in D, both centered at x, with radiuses $r < R$, and call $v_x$ the function $y \to (4\pi)^{-1}(1/|x-y| - 1/R)$. Integrate by parts in the domain O between the two spheres, which can be done in two ways. First, lifting the grad off $v_x$,

$$\begin{aligned}\int_O \mathrm{grad}\,\varphi \cdot \mathrm{grad}\, v_x &= \int_{\partial O} n\,.\,\mathrm{grad}\,\varphi\; v_x \\ &= \tfrac{1}{4\pi}\,(r^{-1} - R^{-1})\int_{S(x,\,r)} n \cdot \mathrm{grad}\,\varphi = \\ &= -\tfrac{1}{4\pi}\,(r^{-1} - R^{-1})\int_{B(x,\,r)} \mathrm{div}(\mathrm{grad}\;\varphi) = 0,\end{aligned}$$

and then, the other way around,

$$\int_O \mathrm{grad}\,\varphi \cdot \mathrm{grad}\, v_x = \tfrac{1}{4\pi}\,[R^{-2}\int_{S(x,\,R)}\varphi - r^{-2}\int_{S(x,\,r)}\varphi].$$

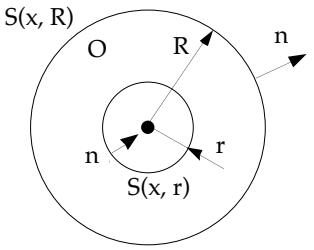


Letting r tend to 0, one finds, finally,

$$\varphi(x) = [\int_{S(x,\,R)}\varphi]/(4\pi R^2), \tag{4}$$

a useful representation formula, which says that $\varphi(x)$ is equal to the average of $\varphi$ over the sphere S(x, R). Of course, $\varphi$ cannot be extremal at x without contradicting this. Hence the maximum principle.

In the case of a non-unifom, but positive permeability, the magnetic potential enjoys a similar property,[5] but the proof ([GT], Chapter 3) is no

[5]This is the basis of Earnshaw's famous result [Ea]: "A charged particle in empty space cannot remain in stable equilibrium under electrostatic forces alone, or alternatively there can be no maximum or minimum of the potential at points free of charge density." (Quoted from [Sc].)

longer elementary. It relies on the intuitive idea that if there was an isolated maximum at $x$, normal fluxes $\mu\, n \cdot \mathrm{grad}\, \varphi$ would all be negative on the surface of a small sphere centered at $x$, thus contradicting flux conservation.

It would be highly unphysical and quite embarrassing indeed if a similar property did not hold for the computed discrete potential, that is, if the potential could surpass I, or be negative, inside D or on $S^b$. *This won't happen if all extra-diagonal terms of* $\mathbf{M}$ *are nonpositive*. Indeed, one can interpret Eq. (2) as the discretized counterpart of (4), as follows:

$$(2') \qquad \boldsymbol{\varphi}_n = \sum \{ m \in \mathcal{N}(n),\, m \neq n :\ (-\mathbf{M}_{nm}/\mathbf{M}_{nn})\, \boldsymbol{\varphi}_m \},$$

showing how $\boldsymbol{\varphi}_n$ is the weighted average of neighboring nodal values. The sum of weights $\sum_{m \neq n} -\mathbf{M}_{nm}/\mathbf{M}_{nn}$ is always equal to 1 (cf. Remark 3.6), but what counts here is the positivity of each of them: If all weights are positive in (2'), then $\boldsymbol{\varphi}_n$ is strictly contained in the interval formed by the minimum and the maximum values of DoFs $\boldsymbol{\varphi}_m$ around it, and thereby,

**Proposition 4.3** ("discrete maximum principle"). *If no extra-diagonal entry of* $\mathbf{M}$ *is positive, the maximum of the approximate potential* $\varphi_m$ *on any cluster* $D_n$ *is reached on its boundary.*

As an immediate corollary, the extrema of $\varphi_m$ on $\overline{D}$ are reached only on the boundary, which is the discrete version of the principle recalled at the beginning of this section.

**Exercise 4.10.** Prove $0 \leq \boldsymbol{\varphi}_n \leq I$ directly from Eq. (3.20), ${}^{00}\mathbf{M}\, {}^{0}\boldsymbol{\varphi} = -{}^{01}\mathbf{M}\, {}^{1}\boldsymbol{\varphi}^{I}$, by using Prop. 3.6.

Nonpositivity of extra-diagonal terms thus appearing as a desirable property, when does it hold, and how can it be achieved? An "acute" mesh (one with no dihedral angle larger than 90°) is enough, as we remarked earlier. But this is a sufficient, not a necessary, condition. What constitutes a necessary and sufficient condition in this respect does not seem to be known, although there is a way in which Voronoi–Delaunay[6] meshes satisfy this requirement. Such meshes have stirred interest in computational electromagnetism [C&, SD, Z&], perhaps because of their apparent (but still not well understood) connection with "network methods" [He], or "finite volume methods" (cf. [Va], p. 191). So let us digress on this for a while.

[6] "Delaunay: This is the French transliteration of the name of Boris Nikolaevitch Delone, who got his surname from an Irish ancestor called Deloney, who was among the mercenaries left in Russia after the Napoleonic invasion of 1812." (J. Conway, `//www.forum.swarthmore.edu/news.archives/geometry.software.dynamic/article49.html`, 15 12 1994.)

### 4.2.2 Voronoi–Delaunay tessellations and meshes

In the plane or space (d = 2 or 3 is the dimension), consider a finite set $\mathcal{N}$ of points, and let domain D, to be meshed, be the interior of their convex[7] hull. The *Voronoi cell* $V_n$ of n is the closed convex set

$$V_n = \{x \in \overline{D} : |x - x_n| \leq |x - x_m| \ \forall m \in \mathcal{N} - \{n\}\}$$

made of points not farther to node n than to any other node. Fig. 4.8 gives an example, with 11 nodes and as many Voronoi cells (the polygons with irregular shapes).

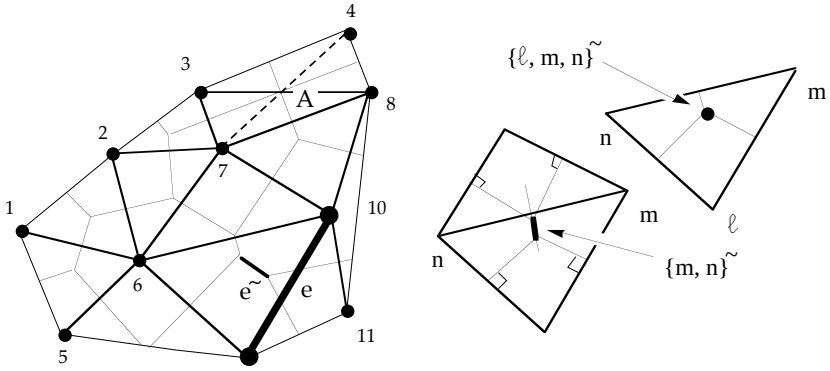


**FIGURE 4.8.** Voronoi-Delaunay mesh in dimension 2. Note the ambiguity about point A and how it is resolved by arbitrarily preferring {3, 8} to {2, 4}. A dual q-cell and the associated (d – q)-simplex are supported by orthogonal and complementary affine subspaces, but do not necessarily encounter each other (like here the edge e and its dual e˜).

These are "d-cells", if one refers to their dimension. One can also define "q-cells" by taking all non-empty intersections of d-cells, two by two (q = d – 1), three by three (q = d – 2), etc. Points of these q-cells are closer to d – q + 1 of the original nodes. For instance, the (d – 1)-cell associated with nodes n and m is

$$V_{n,m} = \{x \in \overline{D} : |x - x_n| = |x - x_m| \leq |x_n - x_k| \ \forall k \in \mathcal{N} - \{n, m\}\},$$

and $x_n$ and $x_m$ are its nearest neighbors among nodes. Generically, p Voronoi cells intersect, if they do, as a convex set of dimension d + 1 – p. There are exceptions: cf. nodes 3 and 8 in Fig. 4.8, where a small segment

[7] Convexity is important, and special precautions must be taken when generating VD meshes for nonconvex regions (cf. [Ge], [We]).

near point A would be made of points closer to 3 and 8, if only 4 and 7 were a little farther away. For simplicity in this description, we shall assume that such degenerate cases are absent (although they can be a nuisance in practice). Voronoi d-cells and their intersections form a cellular tessellation of the domain.

Now let us associate to each of these q-cells the p nodes that define it, $p = d + 1 - q$, that is, nodes which are nearest neighbors to all points of the q-cell. They form a p-simplex, which we shall call a *Dirichlet simplex*. The *Voronoi–Delaunay* (VD) mesh is the simplicial mesh thus obtained. In spite of its being derived from the Voronoi paving, we shall consider the simplicial VD mesh as *primal*, and the system of Voronoi cells as its *dual* cellular mesh, and denote by $\tilde{s}$ the Voronoi cell that corresponds to the primal simplex s. As an example, Fig. 4.8 displays the Voronoi cell $\tilde{e}$ of edge e.

Analogies between this dual and the barycentric one are obvious. From the combinatorial point of view, they are even the same: the dual cells $s^*$ and $\tilde{s}$ are defined by the same set of primal nodes. But the shapes of the cells differ widely. Contrary to $m^*$-cells, Voronoi cells are all convex and lie in a definite affine subspace (of dimension q for q-cells). Compare Figs. 4.4 and 4.9. On the other hand, barycentric duals always intersect their primal associates, whereas Voronoi cells may lie some distance away from their mates (case of e and $\tilde{e}$, Fig. 4.8).

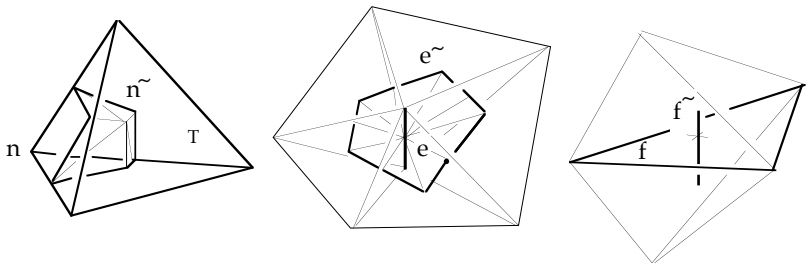


**FIGURE 4.9.** Cells of the Voronoi dual mesh $\tilde{m}$. Compare with Fig. 4.4.

Such VD meshes have remarkable properties. For instance, this, which is an almost immediate consequence of the construction principle:

**Proposition 4.4.** *For each Dirichlet simplex, there is a sphere that contains it and its lower dimensional faces, but no other simplex.*

*Proof.* Take a sphere centered at one of the points of the dual Voronoi cell, of radius equal to the distance to one of the nodes of the simplex

(inset). Other nodes of the simplex, being equidistant, are on the sphere, and all remaining nodes, being farther away, are outside. ◊

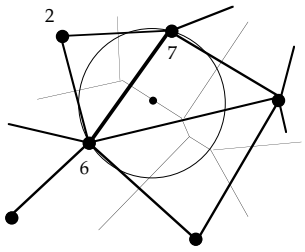


This "sphere property", or circle property in 2D, happens to be characteristic (**Exercise 4.11:** Give an argument to this effect), and is a key-element in incremental VD mesh construction: To add a new vertex to what is already a VD mesh, gather the d-simplices the circumscribed sphere of which contains this vertex, hence a polytope, which is subdivided by joining its vertices to the new vertex. The new mesh is still a VD one [SI, Wa, We].

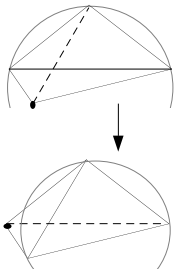

In dimension 2, any triangulation can be transformed into a VD one by successively swapping diagonals of quadrilaterals formed by adjacent triangles. Why this works locally is clear: Angles of quadrilaterals add to $2\pi$, so one of the two diagonals has opposite angles which sum up to less than $\pi$, and a swap will enforce the circle property, as shown in the inset. The difficulty is to prove the *finiteness* of the sequence of swaps [Ch]. (It's due to the swaps decreasing the total area of circumscribed circles [Ni].) Let's finally mention the "maxmin angle property": In dimension 2 again, the VD mesh is the[8] one, among all triangulations with the same node set, that maximizes the smallest angle [RS, SI, Si]. It also minimizes the energy of the finite element solution [RS].

According to [Hr], what we call nowadays a Voronoi cell was introduced in two dimensions by Dirichlet [Di] and in n dimensions by Voronoi [Vo]. (M. Senechal [Se] also gives priority to Dirichlet.) Then came Delaunay [De]. Other names are in use: "Thiessen polygons" among meteorologists[9] [CR], "Dirichlet domains", "Brillouin zones", "Wigner–Seitz cells", etc., among crystallographers.

### 4.2.3 VD meshes and Stieltjes matrices

Now let's come back to the question of nonpositive off-diagonal coefficients. There is an apparently favorable situation in dimension 2:

[8]When there is a *unique* one, of course, which is the generic case, but there are obvious exceptions (Fig. 4.8 shows one).

**Proposition 4.5.** *Assume* $\mu$ *constant in* D. *For all inner nodes* n, $\mathbf{M}_{mn} \le 0$ *for all* $m \neq n$.

*Proof.* Edge mn is flanked by two triangles T and T' (Fig. 4.10), and the opposite angles add up to less than 180°, thanks to the circle property. By the cotangent formula (3.23), $-\mathbf{M}_{mn}$ is proportional to $\cot\theta + \cot\theta'$, which is $\ge 0$ if $\theta + \theta' \le \pi$. ◊

Alas, this leaves many loose strands. First, obtuse angles at boundary triangles (there is one in Fig. 4.8, triangle {8, 10, 11}). But if the objective is to enforce the discrete maximum principle, only inner nodes are involved, and anyway, one may add nodes at the boundary and, if necessary, remesh (which is a local, inexpensive process). Second, and more serious, the condition of uniformity of $\mu$ is overly restrictive, and although the cure is of the same kind (add nodes at discontinuity interfaces to force acute angles), further research is needed in this direction.

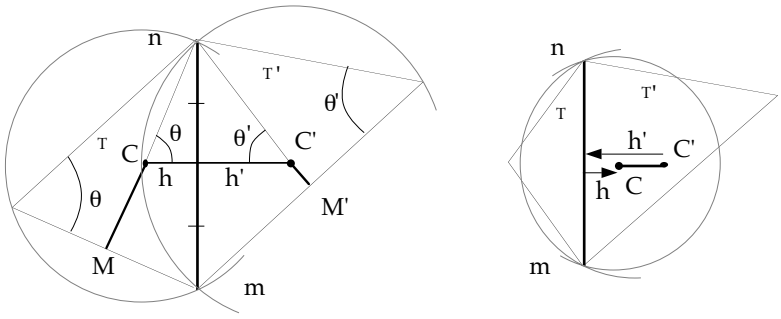


**FIGURE 4.10.** Proof of (5). M and M' are the mid-edges.

Proposition 4.5 can be proven in a different and instructive way (Fig. 4.10). By the cotangent formula, and the obvious angular relation of Fig. 4.10 (where C and C' are the circumcenters), one has

$$(5) \qquad -\mathbf{M}_{mn} = \tfrac{1}{2}\,(\mu(T)\cot\theta + \mu(T')\cot\theta') = (h\,\mu(T) + h'\,\mu(T'))/\,|mn|\,,$$

[9]Conventionally, the conditions reported by a meteorological station (temperature, hygrometry, etc.) are supposed to hold in the whole "Thiessen polygon" around that station. As explained in [CH], "Stations are always being added, deleted, moved, or temporarily dropped from the network when they fail to report for short periods of time (missing data)", hence the necessity to frequently solve the typical problem: having a Voronoi–Delaunay mesh, add or delete a node, and recalculate the boundaries. Recursive application of this procedure is the standard Watson–Bowyer algorithm for VD mesh generation [Wa], much improved recently [SI] by making it resistant to roundoff errors. Fine displays of VD meshes can be found in [We].

where $|mn|$ is the length of edge $\{m, n\}$, and $h$, $h'$ are to be counted algebraically, in the direction of the outward normal (thus, $h \le 0$ if the circumcenter $C$ is outside $T$, as on Fig. 4.10, right part). This way, in the case where $\mu$ is uniform, $\mathbf{M}_{mn} = -\mu\,(h + h')/|mn|$, negative indeed if the circle condition is satisfied.

This quantity happens to be the flux of $\mu$ grad $\lambda^n$ out of the Voronoi cell of node $m$ (**Exercise 4.12:** Prove this, under some precise assumption). This coincidence is explained in inset: Although the Voronoi cell and the barycentric box don't coincide, the flux through their boundaries is the same, because $\mu \nabla\lambda^n$ is divergence-free in the region in between. But beware: Not only does this argument break down when there is an obtuse angle (cf. Exer. 4.12), but it doesn't extend to dimension 3, where circumcenter and gravity center of a face do not coincide.

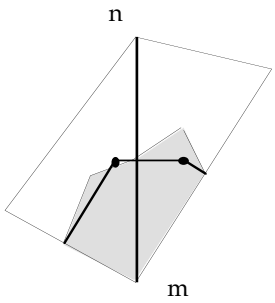


Still, there is some seduction in a formula such as (5), and it *has* a three-dimensional analogue. Look again at Fig. 4.9, middle. The formulas

$$\widetilde{\mathbf{M}}_{mn} = -[\textstyle\sum_F (\text{area}(F)\,\mu(F)]/|mn|, \quad \widetilde{\mathbf{M}}_{nn} = -\sum_{m \in \mathcal{N}} \widetilde{\mathbf{M}}_{mn},$$

where $F$ is an ad-hoc index for the small triangles of the dual cell $\{m, n\}^{\sim}$, do provide negative exchange coefficients between $n$ and $m$, and hence a matrix with Stieltjes principal submatrices. This is a quite interesting discretization method, but not the finite element one, and $\widetilde{\mathbf{M}} \neq \mathbf{M}$.

**Exercise 4.13.** Interpret this "finite volume" method in terms of fluxes through Voronoi cells.

## 4.3 CONVERGENCE AND ERROR ANALYSIS

We now consider a family $\mathcal{M}$ of tetrahedral meshes of a bounded spatial domain D. Does $\varphi_m$ converge toward $\varphi$, in the sense that $\|\varphi_m - \varphi\|_\mu$ tends to zero, when $m \ldots$ when $m$ does *what*, exactly? The difficulty is mathematical, not semantic: We need some structure[10] on the set $\mathcal{M}$ to validly talk about convergence and limit.

[10]The right concept is that of *filter* [Ca]. But it would be pure folly to smuggle that into an elementary course.

The first idea that comes to mind in this respect is to gauge the "coarseness" of $m$, as follows. Let us denote by $\gamma_n(m)$, or simply $\gamma_n$, the maximum distance between $x_n$ and a point of its cluster $D_n$. Call *grain* of the mesh, denoted $\gamma(m)$ or simply $\gamma$, the least upper bound of the $\gamma_n$s, which is also the maximum distance between two points which belong to the same tetrahedron $T$, or maximum *diameter* of the $T$'s.

Now, the statement to prove would seem to be, in the time-honored $\varepsilon$–$\delta$ tradition of calculus, "Given $\varepsilon > 0$, there exists $\delta > 0$ such that, if $\gamma(m) \le \delta$, then $\|\varphi_m - \varphi\|_\mu \le \varepsilon$." Unfortunately, this is plainly *false*. There are straight counter-examples of meshes of arbitrary small grain for which the energy of the computed field stays above the energy minimum by a finite amount: Obtuse angles, larger and larger, do the trick [BA].

What we may expect, however, and which turns out to be true, is the validity of the above statement if the family of meshes is *restricted* by some qualifying conditions. "Acuteness", for instance, defined as the absence of obtuse dihedral angles between any two adjacent faces, happens to work: The statement "Given $\varepsilon > 0$, there exists $\delta > 0$ such that, *if $m$ is acute*, and if $\gamma(m) \le \delta$, then $\|\varphi_m - \varphi\|_\mu \le \varepsilon$" is true (we'll prove it).

Such *convergence* results are essential, because it would make no sense to use the Galerkin method in their absence. But in practice, they are not enough: We should like to know which kind of mesh to build to obtain a prescribed accuracy. Knowing how the above $\delta$ depends on $\varepsilon$ would be ideal: Given $\varepsilon$, make a mesh the grain of which is lower than $\delta(\varepsilon)$. No such general results are known, however, and we shall have to be content with *asymptotic estimates* of the following kind:

$$\|\varphi_m - \varphi\|_\mu \le C\,\gamma(m)^\alpha, \tag{6}$$

where $\alpha$ is a known positive exponent and $C$ a constant[11] which depends on the true solution $\varphi$, but not on the mesh. Again, $C$ cannot be known in advance in general, but (6) tells how *fast* the error will decrease when the grain tends to 0, and this is quite useful. One usually concentrates on the exponent $\alpha$, which depends on the shape functions. Typically, $\alpha = 1$ for the $P^1$ elements.

We shall first present the general method by which estimates like (6) can be obtained, then address the question of which restrictions to force on $\mathcal{M}$ in order to make them valid.

[11]From now on, all $C$'s in error estimates will be constants of this kind, not necessarily the same at different places, which may depend on $\varphi$ (via its derivatives of order 2 and higher, as we shall see), but not on the mesh.

### 4.3.1 Interpolation error and approximation error

Let's develop an idea that was only suggested in Section 2.3.

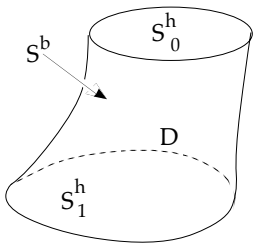


First, a definition: Given a family $\mathcal{M}$ of meshes, an *interpolation procedure* is a similarly indexed family of linear mappings $r_m : \mathcal{U} \to \Phi_m$, where $\mathcal{U}$ is *dense* in $\Phi^*$. Let's give an example immediately: $\mathcal{U}$ is made of all continuous functions over $\overline{D}$ that vanish on $S^h_0$, and its $m$-interpolate is

$$r_m u = \sum_{n \in \mathcal{N}} u(x_n)\, \lambda^n.$$

In other words, $u$ is sampled at nodes, and linearly interpolated in between. This explains why $\mathcal{U}$ cannot coincide with $\Phi^*$ (the complete space), which contains non-continuous functions, for which nodal values may not make sense. In fact, for technical reasons that soon will be obvious, we further restrict $\mathcal{U}$ to piecewise 2-smooth functions that vanish on $S^h_0$. The energy distance $\|u - r_m u\|_\mu = [\int_D \mu\, |\mathrm{grad}(u - r_m u)|^2]^{1/2}$ between a function and its interpolate is called the *interpolation error*.

Next, let's suppose we know something of the same form as (6) about the interpolation error,

$$\|u - r_m u\|_\mu \le C(u)\, \gamma(m)^\alpha. \tag{7}$$

Then, two things may happen. If the true solution $\varphi$ is a member of the class $\mathcal{U}$, the remark of Section 3.3 (cf. Fig. 3.4) about the approximation error $\|\varphi_m - \varphi\|_\mu$ being lower[12] than the interpolation error $\|r_m \varphi - \varphi\|_\mu$ immediately yields (6), with $C = C(\varphi)$. So we may conclude that for meshes of the family for which (7) holds, $r_m \varphi$ converges in energy toward $\varphi$ when the grain tends to 0. Moreover, the speed of the convergence is what the interpolation procedure provides.

This situation does not present itself all the time, however, because the solution may not be smooth enough to belong to $\mathcal{U}$ (cf. the example of Exer. 3.6). But the density of $\mathcal{U}$ still allows us to conclude: Given $\varepsilon$, there exists some $u \in \mathcal{U}$ such that $\|u - \varphi\|_\mu \le \varepsilon/2$, and since

$$\|\varphi_m - \varphi\|_\mu \le \|r_m u - \varphi\|_\mu \le \|r_m u - u\|_\mu + \|u - \varphi\|_\mu,$$

[12]Note that $r_m u \in \Phi^I$ if $u \in \Phi^I$ with the present interpolation procedure, if one turns a blind eye to possible variational crimes at the boundary. This is important in asserting that $\|\varphi_m - \varphi\|_\mu \le \|r_m \varphi - \varphi\|_\mu$.

$\|r_m u - u\|_\mu$ will be smaller that the still unspent half-epsilon for $\gamma(m)$ small enough, hence the convergence. The convergence *speed*, however, is no longer under control. This is not a practical difficulty, because singularities of $\varphi$ are usually located at predictable places (corners, spikes), and special precautions about the mesh (pre-emptive refinement, or special shape functions) can be taken there.

### 4.3.2 Taming the interpolation error: Zlamal's condition

We may therefore concentrate on the interpolation error. By the very definition of hat functions, one has

$$(8) \qquad \sum_{n \in \mathcal{N}} \lambda^n(x)\ (x_n - x) = 0 \quad \forall\, x \in D,$$

which makes sense as a weighted sum of *vectors* $x_n - x$.

Let $u$ be an element of $\mathcal{U}$. We'll make use of its second-order Taylor expansion about $x$, in integral form, as follows:

$$(9) \qquad u(y) = u(x) + \nabla u(x) \cdot (y - x) + \tfrac{1}{2}\ A_u(x, y)(y - x) \cdot (y - x)$$

where, denoting $\partial^2 u$ the matrix of second derivatives of $u$,

$$A_u(x, y) = \int_0^1 (1 - t^2)\ \partial^2 u(x + t(y - x))\ dt,$$

a symmetric matrix that smoothly depends on $x$ and $y$. Note that $\nabla u(x)$ is treated as a vector in (9), and that $A_u$ acts on vector $y - x$.

**Remark 4.3.** The validity of formula (9) is restricted to pairs of points $\{x, y\}$ which are linked by a segment entirely contained in $D$. Not to be bothered by this, we assume $u$ has a smooth extension to the convex hull of $D$. Anyway, only values of $A_u(x, y)$ for points $x$ and $y$ close to each other will matter. ◊

It is intuitive that the distance between $u$ and its interpolate $r_m u$ should depend on the grain in some way. Our purpose is to show that if the mesh is "well behaved", in a precise sense to be discovered, the quadratic semi-norm, which differs only in an inessential way from the energy one,

$$\|u - r_m u\| = [\int_D |\nabla(u - r_m u)|^2]^{1/2},$$

is bounded by $\gamma(m)$, up to a multiplicative constant that depends on $u$ (via its derivatives of order 2).

By Taylor's formula (9), we have, for all node locations $x_n$,

$$u(x_n) = u(x) + \nabla u(x) \cdot (x_n - x) + \tfrac{1}{2}\, A_u(x, x_n)(x_n - x) \cdot (x_n - x).$$

Multiplying this by $\lambda^n$, then using (8) and (9), we see that

$$r_m u(x) = u(x) + \sum_{n \in \mathcal{N}} \lambda^n(x)\, \alpha_n(x),$$

where

$$\alpha_n(x) = \tfrac{1}{2}\, A_u(x, x_n)(x_n - x) \cdot (x_n - x). \tag{10}$$

Therefore,

$$\nabla(r_m u - u) = \sum_{n \in \mathcal{N}} \lambda^n \nabla \alpha_n + \sum_{n \in \mathcal{N}} \alpha_n \nabla \lambda^n. \tag{11}$$

On $D_n$, after (10), $|\nabla \alpha_n|$ is bounded by $\gamma_n$, up to a multiplicative constant. Fields $\lambda^n \nabla \alpha_n$ are thus uniformly bounded by $C\gamma$ on D, and the first term on the right in (11) is on the order of $\gamma(m)$. The one term we may worry about is therefore $\sum_{n \in \mathcal{N}} \alpha_n \nabla \lambda^n$.

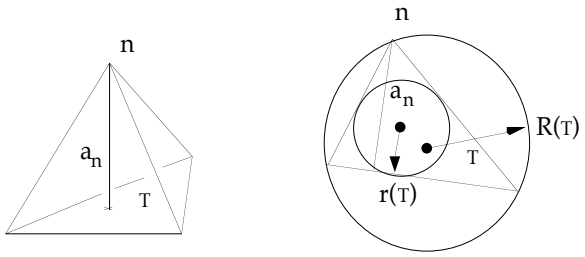


**FIGURE 4.11.** The norm $|\nabla \lambda^n|$ is $1/a_n$, where $a_n$ is the length of the altitude drawn from node n to the opposite face. Right (in 2D for clarity, but this generalizes without problem), the ratio $a_n/\gamma$ is always larger than $r(T)/R(T)$, hence "Zlamal's condition" [Zl]: $R(T)/r(T) \le C$, for all triangles and all meshes in the family. It amounts to the same as requiring that the smallest angle (or in 3D, the smallest dihedral angle) be bounded from below.

And worry we should, for $\nabla \lambda^n$ can become very large: Its amplitude within tetrahedron T is the inverse of the distance $a_n$ from node n to the opposite face in T (Fig. 4.11), so there is no necessary link between $|\nabla \lambda^n|$ and $\gamma_n$. But it's not difficult to establish such a link if the mesh behaves. Remarking that, for x in T (refer to Fig. 4.11, right, for the notation),

$$|x_n - x|\, |\nabla \lambda^n(x)| \le \gamma_n / a_n \le R(T)/r(T),$$

we are led to introduce the dimensionless number

$$A(m) = \sup_{T \in \mathcal{T}(m)} R(T)/r(T)$$

(maximum ratio of radii of the circumscribed and inscribed spheres), which measures the global "angle acuteness" of the mesh, as explained under Fig. 4.11. Then

$$|\sum_{n \in \mathcal{N}} \alpha_n(x)\, \nabla\lambda^n(x)| \le C \sum_{n \in \mathcal{N}} \gamma_n |x_n - x|\ |\nabla\lambda^n(x)|$$
$$\le CA(m)\,\gamma(m).$$

So then, the second term on the right in (11) also is in $\gamma(m)$, and we have, whatever x,

$$|\nabla(r_m u - u)(x)| \le C\,A(m)\,\gamma(m). \tag{12}$$

Integrating (12) over the bounded domain D, we find that

$$\sup_m A(m) < \infty \Rightarrow \|u - r_m u\| \le C(D, u)\,\gamma(m). \tag{13}$$

Hence our first result: For a family of meshes with bounded acuteness, there is convergence when the grain tends to 0, and the exponent $\alpha$ in (7) is equal to 1.

The existence of such an upper bound for acuteness is equivalent to Zlamal's famous "angle condition" (Fig. 4.11): All angles, for all meshes in the family, should be bounded from below by a fixed, positive amount.

### 4.3.3 Taming the interpolation error: Flatness

But the rough way by which we obtained estimates suggests that Zlamal's condition may be too strong. Actually, very early in the practice of finite elements, it was clear from experience that acute angles were not necessarily "bad". Besides, as we saw with Exercises 3.14 and 3.15, there is a way to recover finite difference schemes from finite element approximations by using a regular orthogonal mesh and by halving rectangles, in dimension 2, or dissecting hexahedra into tetrahedra, in dimension 3. The approximation theory for such finite difference schemes was well-established at the beginning of the finite element era, and it showed no trace of an "acute angle condition", which strongly suggested that Zlamal's condition was too strong indeed.

It took some time, however (in spite of an early remark by Synge [Sy]), before the condition was properly relaxed, and replaced, in dimension 2, by a *maximum* angle condition, with counter-examples showing that obtuse angles were effectively detrimental [BA], and a more accurate condition

(less intuitive than Zlamal's criterion, unfortunately) was formulated [Ja]. The current state of the art can be summarized informally like this: "If the error is too large, or if convergence rate seems poor, don't blame it on acute angles. Watch out for *obtuse* angles instead."

To make this more precise, let us try and improve on the above estimate, as follows. We have, using $\lambda^n = 1 - \sum_{m \neq n} \lambda^m$ to pass from line 2 to line 3 of the following string of equalities, and imbedding $\mathcal{E}$ in $\mathcal{N} \times \mathcal{N}$ the obvious way,

$$\begin{aligned}
\|\textstyle\sum_{n \in \mathcal{N}} \alpha_n \nabla\lambda^n\|^2 &= \textstyle\int_D |\sum_{n \in \mathcal{N}} \alpha_n \nabla\lambda^n|^2 \\
&= \textstyle\sum_{n \in \mathcal{N},\, m \in \mathcal{N}} \int_D \alpha_n \alpha_m \nabla\lambda^n \cdot \nabla\lambda^m \\
&= \textstyle\sum_{n \neq m} \int_D \alpha_n \alpha_m \nabla\lambda^n \cdot \nabla\lambda^m - \sum_{n \neq m} \int_D \alpha_n^2 \nabla\lambda^n \cdot \nabla\lambda^m \\
&= \textstyle\sum_{n \neq m} \int_D \alpha_n (\alpha_m - \alpha_n) \nabla\lambda^n \cdot \nabla\lambda^m \\
&= -\textstyle\sum_{\{m,\, n\} \in \mathcal{E}} \int_D (\alpha_m - \alpha_n)^2 \nabla\lambda^n \cdot \nabla\lambda^m \\
&= -\textstyle\sum_{T \in \mathcal{T}} \int_T \sum_{\{m,\, n\} \in \mathcal{E}(T)} (\alpha_m - \alpha_n)^2 \nabla\lambda^n \cdot \nabla\lambda^m .
\end{aligned}$$

As $\alpha_m - \alpha_n = \frac{1}{2} A_u(x_m - x) \cdot (x_m - x) - \frac{1}{2} A_u(x_n - x) \cdot (x_n - x)$ (up to terms of higher order), one has, with the same degree of approximation, $\alpha_m - \alpha_n \sim \frac{1}{2} A_u(x_m - x_n) \cdot (x_n + x_m - 2x)$, hence the estimate

$$|\alpha_m - \alpha_n| \leq C\gamma_n |x_m - x_n| .$$

Let us therefore introduce the dimensionless quantity

$$F(m) = \sup_{T \in \mathcal{T}} [\textstyle\int_T \sum_{\{m,\, n\} \in \mathcal{E}(T)} |x_n - x_m|^2 \, |\nabla\lambda^n \cdot \nabla\lambda^m| \, / \mathrm{vol}(T)]^{1/2} \tag{14}$$

and call it "flatness" of the mesh. Then,

$$\|\textstyle\sum_{n \in \mathcal{N}} \alpha_n \nabla\lambda^n\|^2 \leq C \gamma(m)^2 F(m)^2 \sum_{T \in \mathcal{T}} \mathrm{vol}(T),$$

so we may conclude:

$$\sup_m F(m) < \infty \Rightarrow \|u - r_m u\| \leq C(D, u) \gamma(m) . \tag{15}$$

By limiting flatness, thus, one makes sure the interpolation error will tend to zero with the mesh grain, just as one did by limiting acuteness, via Zlamal's criterion.

But flatness, in this respect, is a better criterion than acuteness, for controlling the latter amounted to bounding $|\nabla\lambda^n| \, |\nabla\lambda^m|$ instead of $|\nabla\lambda^n \cdot \nabla\lambda^m|$. When evaluating flatness, near orthogonality of $\nabla\lambda^n$ and

$\nabla\lambda^m$ is acknowledged as a favorable factor (cf. the cotangent formula), which the acuteness criterion ignores.

Still, what we have in (14) is only an algebraic figure of merit, not yet formally linked with the shape of the tetrahedra. We now prove that a ban on obtuse angles does limit flatness (and hence, since (15) applies, is a sufficient, though not necessary condition for convergence).

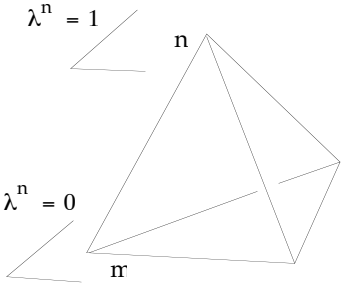


**Lemma 4.1.** *One has* $mk \cdot \nabla\lambda^n = 0$ *unless* $n = k$ *or* $m$, *and* $mn \cdot \nabla\lambda^n = 1$.

*Proof.* The circulation of $\nabla\lambda^n$ along edge $\{m, k\}$ is $mk \cdot \nabla\lambda^n$. On the other hand, the circulation of $\nabla\lambda^n$ along any line is the difference of values of $\lambda^n$ at its ends (inset), and $\lambda^n$ vanishes at all nodes except n, where it takes the value 1. ◊

**Proposition 4.6.** *In spatial dimension* $d$, *one has*

$$-\sum_{\{m,\,n\}\in\mathcal{E}(T)} |x_n - x_m|^2\, \nabla\lambda^n \cdot \nabla\lambda^m = d. \tag{17}$$

*Proof.* The proof is easy if $d = 2$, and we sketch it for $d = 3$. Start from the following identity (Jacobi's),

$$kn \times (k\ell \times km) + k\ell \times (km \times kn) + km \times (kn \times k\ell) = 0,$$

which entails $kn \times \nabla\lambda^n + k\ell \times \nabla\lambda^\ell + km \times \nabla\lambda^m = 0$. Square this, using the identity $(a \times b) \cdot (c \times d) = a \,.\, c\; b \,.\, d - a \,.\, d\; b \,.\, c$, and Lemma 4.1. Square terms give things like $|kn|^2\, |\nabla\lambda^n|^2 - 1$ and rectangle terms contribute factors like

$$\begin{aligned} 2\,(kn \times \nabla\lambda^n) \cdot (km \times \nabla\lambda^m) &= 2\, kn \cdot km\;\; \nabla\lambda^n \cdot \nabla\lambda^m \\ &= (mn^2 - km^2 - kn^2)\; \nabla\lambda^n \cdot \nabla\lambda^m. \end{aligned}$$

Adding all that yields (17). ◊

**Corollary.** *If all dihedral angles are acute, then*

$$\|u - r_m u\| \le C(D, u)\, \gamma(m).$$

*Proof.* Then all coefficients $\nabla\lambda^n \cdot \nabla\lambda^m$ are negative, and therefore

$$\begin{aligned} \Big\|\sum_{n\in\mathcal{N}} \alpha_n \nabla\lambda^n\Big\|^2 &\le -C \sum_{T\in\mathcal{T}} \sum_{\{m,\,n\}\in\mathcal{E}(T)} \int_T (\alpha_m - \alpha_n)^2\, \nabla\lambda^n \cdot \nabla\lambda^m \\ &\le -C\, \gamma(m)^2 \sum_{T\in\mathcal{T}} \mathrm{vol}(T) \sum_{\{m,\,n\}\in\mathcal{E}(T)} |x_n - x_m|^2\, \nabla\lambda^n \cdot \nabla\lambda^m \end{aligned}$$

$$\leq dC\,\gamma(m)^2 \sum_{T \in \mathcal{T}} \mathrm{vol}(T) \equiv dC\,\gamma(m)^2\ \mathrm{vol}(D). \quad \Diamond$$

Thus, acute meshes have all virtues: well-behaved interpolation error, and enforcement of the discrete maximum principle. A pity they are so difficult to produce!

Anyway, there is something disappointing in all these error estimates and convergence criteria: Nowhere did we find any indication on how to compute *upper bounds* on the approximation error, either a priori (but let's not dream) or a posteriori. So the simple and so important question, "how far apart are $\varphi$ and $\varphi_m$ ?" is still unanswered. We'll find a way in this direction in Chapter 6. But before that, we need improved mathematical equipment.

## EXERCISES

Exercises 4.1, 4.2, and 4.3 are on pp. 96, 99, and 100, respectively.

**Exercise 4.4.** Suppose the problem consists in finding $\varphi$ in $\Phi^0$ such that $\int_D \mu\ \mathrm{grad}\,\varphi \cdot \mathrm{grad}\,\varphi' = \int_D f\,\varphi' + \int_S g\,\varphi' \quad \forall\ \varphi' \in \Phi^0$. Use the "flux accounting" idea to find the discrete equations directly.

Exercises 4.5 to 4.9 are on pp. 103 to 105, Exer. 4.10 is on p. 106, and Exers. 4.11 to 4.13 are on pp. 109 to 111.

## HINTS

4.1. Cf. Exer. 3.7 for the cube. But you will see the result does not depend on which way the cube is partitioned.

4.2. Use (2), with obvious changes to cater for dimension 2: 1/2 instead of 1/3, etc., and sum over the nodes of the subset list. The most effective way to proceed may be to label all edge sides, as in Fig. 4.12 below, and to work out the algebraic relations implied by (3) between outward fluxes. Remember that fluxes across the whole boundary of an element must vanish.

4.3. Edges must be neighbors, but this can happen in two ways: by sharing a node (then both belong to some face), or not (then both belong to some tetrahedron). Draw the parts of the 2-cells inside a single tetrahedron in order to visualize the intersection.

4.4. Data $f$ and $g$ are flux loss densities, so their integrals over boxes, or in the case of $g$, the part of the box's boundary that lies in $S$, balance inter-box exchanges.

4.5. Apply Prop. 4.2 to $b - \mu_0 m$.

4.6. $\Sigma_1$ does not bound modulo $S^b$, but the union of *two* such surfaces does, hence the equality of fluxes through each of them.

4.7. Since $(\mathbf{M}\boldsymbol{\varphi})_n$ has the dimensions of a flux, whereas $-\operatorname{div}(\mu \operatorname{grad} \varphi)$ is a flux *density*, introduce the volume of the box $B_n$.

4.8. Call ${}^h\boldsymbol{\varphi}$ the vector of nodal values on $S^h$, and use the same block forms as in Section 3.3.3, with $\boldsymbol{\varphi} = \{{}^0\boldsymbol{\varphi}, {}^h\boldsymbol{\varphi}\}$. Observe that $\int_D \mu\, |\operatorname{grad} \varphi|^2 = \int_S \mu\, \partial_n \varphi\, \varphi^h = \int_{S^h} \mu\, P\varphi^h\, \varphi^h$, where $P$ is a certain linear operator. The aim of the exercise is thus to work out the discrete analogue of this operator. How does it relate with the reluctance of the region, "as seen from the boundary"?

4.9. Work on $x \to 1/|x|$, and remember $\operatorname{div}(\varphi u) = \varphi \operatorname{div} u + \nabla\varphi \cdot u$.

4.10. Show that ${}^0\boldsymbol{\varphi} \geq 0$ first, then work on the translate $\boldsymbol{\varphi} - I$ to show that ${}^0\boldsymbol{\varphi} \leq I$, by the same method.

4.11. Suppose a non-Delaunay tetrahedron is in the mesh. Show that its circumscribed sphere must contain other nodes.

4.12. Note that the flux density through CC' is $1/|mn|$. Treat separately segments CC' and MC, M'C', of the cell boundary. Beware the obtuse angle.

4.13. Same as Exer. 4.12, if all circumcenters are inside tetrahedra.

## SOLUTIONS

4.1. Tetrahedron: $\chi = 4 - 6 + 4 - 1 = 1$. Cube without inner edge: $\chi = 8 - 18 + 16 - 5 = 1$. With one: $\chi = 8 - 19 + 18 - 6 = 1$.

4.2. The following pedestrian solution works convincingly. Call $F_k$ the outgoing flux at edge $k$, with the labelling of Fig. 4.12. One has $F_2 + F_{11} + F_{12} = 0$, and eight other similar relations. Add them all, which results in $\sum_{1 \leq k \leq 27} F_k = 0$. On the other hand, relation (2) expressed at nodes $i$ and $j$ implies $\sum_{8 \leq k \leq 17} F_k + F_{26} + F_{27} = 0$ and $\sum_{18 \leq k \leq 25} F_k + F_{26} + F_{27} = 0$ respectively. Add these, and subtract the previous one, hence $2(F_{26} + F_{27}) = \sum_{1 \leq k \leq 7} F_k$, which is the flux exiting from $\Sigma_1$. But $F_{26} + F_{27}$ is one of the "flux leaks", which has no reason to vanish. (If that accidentally happened, a slight perturbation in the nodal positions would restore the

generic situation.) The case on the right is similar: The flux exiting from $\Sigma_2$ is the sum of flux leaks at the perimeter of T, that is, $\sum_{1 \le k \le 6} F_k$. Subtract $F_1 + F_2 + F_3$, which is 0, and what remains, $F_4 + F_5 + F_6$, again does not vanish, generically.

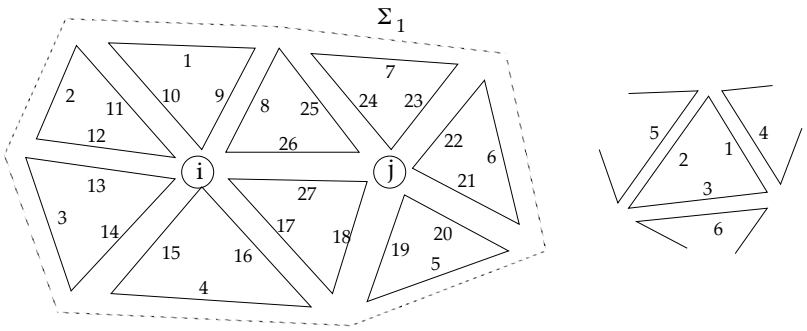


**FIGURE 4.12.** Ad-hoc edge numberings for Exer. 4.2.

4.3. Figure 4.13.

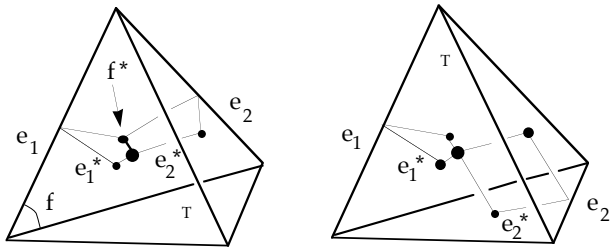


**FIGURE 4.13.** How dual 2-cells can intersect. Left: Edges $e_1$ and $e_2$ have a common node, and define face f. Then $e_1^*$ and $e_2^*$ intersect along $f^*$. Right: they belong to the same tetrahedron, but without any common node. Then $e_1^* \cap e_2^*$ is the barycenter of T.

4.4. Define $\mathbf{f}_n = \int_{B_n} f$ and $\mathbf{g}_n = \int_{S \cap \partial B_n} g$. Then box $B_n$ receives $(\mathbf{M}\boldsymbol{\varphi})_n$ from adjacent boxes and loses $\mathbf{f}_n + \mathbf{g}_n$. The linear system to solve is thus $\mathbf{M}\boldsymbol{\varphi} = \mathbf{f} + \mathbf{g}$. The equations are identical if f and g are approximated by mesh-wise affine functions.

4.7. Let us denote by $\mathbf{V}_n$ the volume of the box $B_n$ and by $\mathbf{V}$ the diagonal matrix of the $\mathbf{V}_n$'s. Since $(\mathbf{M}\boldsymbol{\varphi})_n$ is the "flux loss at n", the term $(\mathbf{M}\boldsymbol{\varphi})_n/\mathbf{V}_n$ can be dubbed the "flux loss *density* about n". Since, on the other hand, $\int_{\Sigma_n} n \,.\, b = \int_{\Sigma_n} \mu\, n \cdot \mathrm{grad}\, \varphi = \int_{B_n} \mathrm{div}(\mu\, \mathrm{grad}\, \varphi)$, this flux-loss density is

– div(μ grad φ) in the continuous case. The matrix equivalent of – div(μ grad ), therefore, is not $\mathbf{M}$ but $\mathbf{V}^{-1}\mathbf{M}$.

4.8. Let's do things formally: $\Phi^h$ is the functional space $\{\varphi \in \Phi : \varphi = \varphi^h \text{ on } S^h\}$, and $\varphi$ satisfies $\int_D \mu \text{ grad } \varphi \cdot \text{grad } \varphi' = 0 \ \ \forall\, \varphi' \in \Phi^0$. This solution linearly depends on the data $\varphi^h$, hence a linear map $P : \varphi^h \to \mu\, \partial_n \varphi$. Now, integrating by parts,[13] $\int_D \mu\, |\text{grad } \varphi|^2 = \int_{S^h} P\varphi^h\, \varphi^h$. The best estimate of this is $(\mathbf{M}\boldsymbol{\varphi}, \boldsymbol{\varphi})$, as evaluated by taking account of the relation ${}^{00}\mathbf{M}\,{}^0\boldsymbol{\varphi} + {}^{01}\mathbf{M}\,{}^h\boldsymbol{\varphi} = 0$. Therefore,

$$(\mathbf{M}\boldsymbol{\varphi}, \boldsymbol{\varphi}) = ({}^{10}\mathbf{M}\,{}^0\boldsymbol{\varphi} + {}^{11}\mathbf{M}\,{}^h\boldsymbol{\varphi},\, {}^h\boldsymbol{\varphi}) = ([{}^{11}\mathbf{M} - {}^{10}\mathbf{M}({}^{00}\mathbf{M})^{-1}\,{}^{01}\mathbf{M}]\,{}^h\boldsymbol{\varphi},\, {}^h\boldsymbol{\varphi})$$

$$= (\mathbf{P}\,{}^h\boldsymbol{\varphi},\, {}^h\boldsymbol{\varphi}).$$

The variationally correct approximation of P, accordingly, is found to be $\mathbf{P} = {}^{11}\mathbf{M} - {}^{10}\mathbf{M}({}^{00}\mathbf{M})^{-1}\,{}^{01}\mathbf{M}$. In case of one mmf I, reluctance R is related with the magnetic coenergy by $\int_D \mu\, |\text{grad } \varphi|^2 = I^2/R$. Matrix $\mathbf{P}$ is thus the inverse of a "multipolar inductance", by which the region can been treated as an inductive circuit element, in some higher-level modelling.

4.9. First, $\text{grad}(x \to |x|^2) = x \to 2x$, and therefore, $\text{grad}(x \to |x|^\alpha) = x \to \alpha\, |x|^{\alpha-2} x$. In particular (and of constant usefulness), the gradient of $x \to |x|$ is $x \to x/|x|$ and $\text{grad}(x \to 1/|x|) = x \to -x/|x|^3$. Now, $\text{div}(x \to x) = 3$, by Exer. 1.3, thus

$$\Delta(x \to 1/|x|) = x \to [-3/|x|^3 + 3x \cdot x/|x|^5] \equiv 0 \text{ if } x \neq 0.$$

4.10. All entries of ${}^{01}\mathbf{M}$ are off-diagonal in $\mathbf{M}$, so $-{}^{01}\mathbf{M}\,{}^1\boldsymbol{\varphi}^I \geq 0$, in the notation of Chapter 3. The principal submatrix ${}^{00}\mathbf{M}$ is Stieltjes, hence ${}^0\boldsymbol{\varphi} = -({}^{00}\mathbf{M})^{-1}\,{}^{01}\mathbf{M}\,{}^1\boldsymbol{\varphi}^I \geq 0$. Now invert the roles of boundaries $S^h_0$ and $S^h_1$, setting $\boldsymbol{\varphi} - I = 0$ on $S^h_1$ and $-I$ on $S^h_0$, hence all potentials $\leq I$ by the same reasoning.

4.11. If a tetrahedron is retained in the VD mesh, it's because there is a set of points which are closer to its vertices than to all other nodes, and this set contains the center of the circumscribed sphere. So this center is closer to another node if the tetrahedron was not Delaunay to start with. (One may apply the same reasoning to all simplices, not only those of maximum dimension: Introduce the "mediator set" of a subset of nodes, as the set of points equidistant to all of them, and center circumscribed spheres on points of this set.)

[13] All this implicitly assumes some regularity, but the reader is encouraged to ignore such issues, which will be addressed in earnest in Chapter 7.

4.12. Since $\mu\nabla\lambda^n = 0$ out of $T \cup T'$, the flux to consider is through the broken line MCC'M'. But since $\nabla\lambda^n$ is parallel to MC and M'C', what remains is the flux through CC', which is $\mu\,(h + h')/|mn|$. The whole thing breaks down if one of the circumcenters, C for instance, is outside its triangle, for then $\nabla\lambda^n$ is not parallel to the part of MC lying inside $T'$.

4.13. If all circumcenters are inside tetrahedra, this is the box-method, relative to Voronoi boxes.

## REFERENCES


[BA] I. Babuš ka, A.K. Aziz: "On the angle condition in the finite element method", **SIAM. J. Numer. Anal., 13**, 2 (1976), pp. 214–226.

[Ca] H. Cartan: "Théorie des filtres", **C.R. Acad. Sc. Paris, 205** (1937), pp. 595–598.

[C&] Z.J. Cendes, D. Shenton, H. Shahnasser: "Magnetic Field Computation Using Delaunay Triangulation and Complementary Finite Element Methods", **IEEE Trans, MAG-19**, 6 (1983), pp. 2551–2554.

[CS] M.V.K. Chari, P. Silvester: "Finite Element Analysis of Magnetically Saturated D–C Machines", **IEEE Trans., PAS-90,** 5 (1971), pp. 2362–2372.

[Ch] C. Cherfils, F. Hermeline: "Diagonal swap procedures and characterization of Delaunay triangulations", **M2AN, 24**, 5 (1990), pp. 613–625.

[CR] A.K. Cline, R.L. Renka: "A storage-efficient method for construction of a Thiessen triangulation", **Rocky Mountain J. Math., 14,** 1 (1984), pp. 119–139.

[CH] T.E. Croley II, H.C. Hartmann: "Resolving Thiessen Polygons", **J. Hydrology, 76** (1985), pp. 363–379.

[De] B. Delaunay: "Sur la sphère vide", **Bull. Acad. Sci. URSS, Class. Sci. Math. Nat**. (1934), pp. 793–800.

[Di] G.L. Dirichlet: "Über die Reduction der positiven quadratischen Formen mit drei unbestimmten ganzen Zahlen", **J. Reine Angew. Math., 40** (1850), p. 209.

[Ea] S. Earnshaw (1805–1888): "On the Nature of the Molecular Forces which Regulate the Constitution of the Luminiferous Ether", **Trans. Cambridge Phil. Soc., 7** (1842), pp. 97–114.

[EF] E.A. Erdelyi, E.F. Fuchs: "Fields in Electrical Devices Containing Soft Nonlinear Materials", **IEEE Trans., MAG-10,** 4 (1974), pp. 1103–1108.

[FE] E.F. Fuchs, E.A. Erdelyi: "Nonlinear Theory of Turboalternators—Pt. I", **IEEE PES Summer Meeting**, San Francisco, July 9–14 (1972), pp. 583–599.

[Ge] P.L. George: **Génération automatique de maillages. Applications aux méthodes d'éléments finis,** Masson (Paris), 1990.

[GT] D. Gilbarg, N.S. Trudinger: **Elliptic Partial Differential Equations of Second Order,** Springer-Verlag (Berlin), 1977.

[GH] M.J. Greenberg, J.R. Harper: **Algebraic Topology, A First Course**, Benjamin/ Cummings (Reading, MA), 1981.

[He] B. Heinrich: **Finite Difference Methods on Irregular Networks**, Akademie-Verlag (Berlin), 1987.

[Hr] F. Hermeline: "Triangulation automatique d'un polyèdre en dimension N", **RAIRO Analyse Numérique, 16**, 3 (1982), pp. 211–242.

[HW] P.J. Hilton, S. Wylie: **Homology Theory,** An Introduction to Algebraic Topology, Cambridge U.P. (Cambridge), 1965.

[Ja] P. Jamet: "Estimations d'erreur pour des éléments finis droits presque dégénérés", **RAIRO Anal. Numer., 20** (1976), pp. 43–61.

[Ni] G.M. Nielson: "A criterion for computing affine invariant triangulations", **IMACS 88**, pp. 560–562.

[RS] S. Rippa, B. Schiff: "Minimum energy triangulations for elliptic problems", **Comp. Meth. Appl. Mech. Engng., 84** (1990), pp. 257–274.

[SD] Y. Saito, S. Ikeguchi, S. Hayano: "An Efficient Computation of Saturable Magnetic Field Problem Using Orthogonal Discretization", **IEEE Trans., MAG-24**, 6 (1988), pp. 3138–3140.

[Sc] W.T. Scott: "Who Was Earnshaw?", **Am. J. Phys., 27**, 4 (1959), pp. 418–419.

[Se] M. Senechal: **Crystalline Symmetries,** An informal mathematical introduction, Adam Hilger (Bristol), 1990.

[Si] R. Sibson: "Locally equiangular triangulations", **The Computer Journal, 21,** 3 (1978), pp. 243–245.

[SI] K. Sugihara, M. Iri: "A robust topology-oriented incremental algorithm for Voronoi diagrams", **Int. J. Comp. Geometry & Appl., 4,** 2 (1994), pp. 179–228.

[Sy] J. L. Synge: **The Hypercircle in Mathematical Physics**, Cambridge U.P. (Cambridge), 1957.

[Va] R.S. Varga: **Matrix Iterative Analysis**, Prentice-Hall (Englewood Cliffs, NJ), 1962.

[Vo] G. Voronoi: "Nouvelles applications des paramètres continus à la théorie des formes quadratiques: recherches sur les parallélоèdres primitifs", **J. Reine Angew. Math., 134** (1908), pp. 198–287.

[Wa] D.F. Watson: "Computing the *n*-dimensional Delaunay tessellation with application to Voronoi polytopes", **Comp. J., 24,** 2 (1981), pp. 167–72.

[We] N.P. Weatherhill: "A method for generating irregular computational grids in multiply connected domains", **Int. J. Numer. Meth. Fluids, 8** (1988), pp. 181–97.

[Z&] Zhou Jian-ming, Shao Ke-ran, Zhou Ke-ding, Zhan Qiong-hua: "Computing constrained triangulation and Delaunay triangulation: A new algorithm", **IEEE Trans**., **MAG-26**, 2 (1990), pp. 694–7.

[Zl] M. Zlamal: "On the finite element method", **Numer. Math., 12** (1968), pp. 394–409.